



## Supporting Information

for *Small*, DOI: 10.1002/smll.202107743

New Insights into Phase-Mechanism Relationship of  
 $\text{Mg}_x\text{MnO}_2$  Nanowires in Aqueous Zinc-Ion Batteries

*Zhongzhuo Yang, Xuelei Pan, Yuanhao Shen, Renpeng  
Chen, Tianzhao Li, Lin Xu,\* and Liqiang Mai*

## Supporting Information

### **New Insights into Phase-Mechanism Relationship of $Mg_xMnO_2$ Nanowires in Aqueous Zinc-Ion Batteries**

*Zhongzhuo Yang, Xuelei Pan, Yuanhao Shen, Renpeng Chen, Tianzhao Li, Lin Xu,\* and Liqiang Mai*

Z. Yang, X. Pan, Y. Shen, R. Chen, T. Li, Prof. L. Xu, Prof. L. Mai  
State Key Laboratory of Advanced Technology for Materials Synthesis and Processing,  
School of Materials Science and Engineering, Wuhan University of Technology, Wuhan  
430070, P. R. China

Prof. L. Xu, Prof. L. Mai  
Foshan Xianhu Laboratory of the Advanced Energy Science and Technology Guangdong  
Laboratory; Xianhu hydrogen Valley, Foshan 528200, China  
E-mail: [linxu@whut.edu.cn](mailto:linxu@whut.edu.cn) (Prof. L. Xu)

## Experimental Section

### *Materials synthesis:*

**Materials:** The chemicals in this work were all commercially available and used as received. Hydrogen peroxide ( $\text{H}_2\text{O}_2$ , 30%), manganese sulfate monohydrate ( $\text{MnSO}_4 \cdot \text{H}_2\text{O}$ , 99%), sodium hydroxide (NaOH, 96%), magnesium chloride hexahydrate ( $\text{MgCl}_2 \cdot 6\text{H}_2\text{O}$ , 98%), zinc sulfate heptahydrate ( $\text{ZnSO}_4 \cdot 7\text{H}_2\text{O}$ , 99.5%) and glacial acetic acid ( $\text{CH}_3\text{COOH}$ , 99.5%) were obtained from Sinopharm Chemical Reagent Co. Ltd., China. Manganese nitrate tetrahydrate ( $\text{Mn}(\text{NO}_3)_2 \cdot 4\text{H}_2\text{O}$ , 98%) was purchased from Macklin. Potassium chlorate ( $\text{KClO}_3$ , 99.5%) was obtained from Aladdin.

**Synthesis of  $\text{Mg}_x\text{MnO}_2$ :**  $\text{Mg}_x\text{MnO}_2$  was synthesized by three steps. Firstly, Na-birnessite precursor was prepared: Two solutions were made, with solution 1 consisting of 50 mL of combined 1 g NaOH and 5 mL  $\text{H}_2\text{O}_2$  and solution 2 consisting of 25 mL of 1.9 g  $\text{Mn}(\text{NO}_3)_2$ . Solution 1 was quickly poured into solution 2 under fast stirring. After mixing, the solution was aged for 96 hours at room temperature. The precipitate was then filtered out of solution and washed several times with deionized water. Secondly, Mg-buserite was formed by ion-exchange reaction: The centrifuged Na-birnessite was transferred to 1 M  $\text{MgCl}_2$  solution under stirring for 24 h. This ion-exchange reaction was repeated three times. Mg-buserite was collected after filtration, washed thoroughly and dried in oven for 8 hours. Finally, the  $\text{Mg}_x\text{MnO}_2$  was obtained: 100 mg of Mg-buserite was added to 17 mL of 1 M  $\text{MgCl}_2$ , the solution is transferred into a 50 mL Teflon-lined stainless-steel autoclave, and treated at 220 °C for 96 hours. After cooling, the product was achieved by centrifugation several times with deionized water and then dried at 60 °C in the oven.

**Synthesis of  $K_xMnO_2$ :** Firstly, 2 mmol  $MnSO_4 \cdot H_2O$ , 3.5 mmol  $KClO_3$  and 3.5 mmol  $CH_3COOK$  were homogeneously dissolved in 35 ml deionized water with constant stirring. Then, the 1.6 mL  $CH_3COOH$  was added into the above solution. After that, the homogeneous solution was transferred into a 50 mL Teflon-lined stainless-steel autoclave and heated at 160 °C for 12 h. After cooling down to room temperature naturally, the sample was washed by water and ethanol for three times and dried at 60 °C in the oven.

***Materials characterization:***

XRD patterns were recorded by using a D2 discover X-ray diffractometer with Cu  $K\alpha$  radiation. The Raman spectra were acquired with an excitation laser of 532 nm by Horiba LabRAM HR Evolution. X-ray photoelectron spectroscopy (XPS) spectra were recorded using a VG MultiLab 2000 instrument. The transmission electron microscopy (TEM) and scanning electron microscopy (SEM) images were taken on JEM-2100F STEM/EDS microscope and JEOL-7100F SEM microscope, respectively. The XAFS data of the Mn K-edge were collected on BL11B beamline of Shanghai Synchrotron Radiation Facility (SSRF) and analyzed with software of Ifeffit Athena<sup>[1]</sup>.

***Electrochemical Measurements:***

The working cathode was composed of active materials (70 wt%), acetylene black conductive additive (20 wt%) and polyvinylidene fluoride (PVDF) (10 wt%). The homogenous ink was casted on carbon paper and dried at 60 °C overnight. After that, the carbon paper was punched into round sheets with a diameter of 10 mm as cathode. 2032 coin cells were assembled with cathode, glass fiber filter paper as separator, zinc metal foil as anode. 2 M  $ZnSO_4$  + 0.2 M  $MnSO_4$  and 2 M  $ZnSO_4$  aqueous solution served as the electrolyte, respectively. Galvanostatic

charge/discharge tests were undertaken on a multi-channel battery testing system (LAND CT2001A) with a cutoff voltage of 1.0-1.8 V vs.  $\text{Zn}^{2+}/\text{Zn}$ . Additionally, CV and electrochemical impedance spectroscopy were conducted with EC-LAB. The SPEIS was recorded using an electrochemical workstation: A potential sweep is made from  $E_i = 1.0$  V to  $E_f = 1.8$  V with the potential decrease of 5 mV followed by 15 min rest per step. On each step, an impedance measurement is performed for a whole frequency range from  $f_i=100$  kHz to  $f_f=0.01$  Hz with 71 points. There are 320 EIS plots during the whole discharge/charge processes. Take a plot for every 10 plots to make a picture. All the tests were carried out at room temperature.

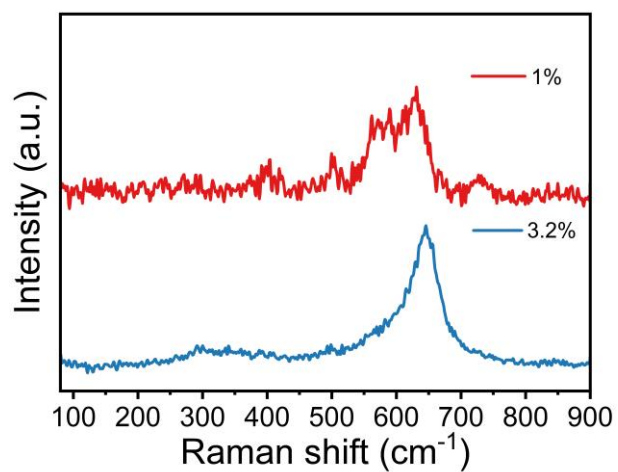


**Figure S1.** Raman spectra of  $\text{Mg}_x\text{MnO}_2$  under different laser illumination at 532 nm.

$\text{Mg}_x\text{MnO}_2$  is more susceptible to laser illumination, so it is necessary to choose a suitable

laser wavelength and power.

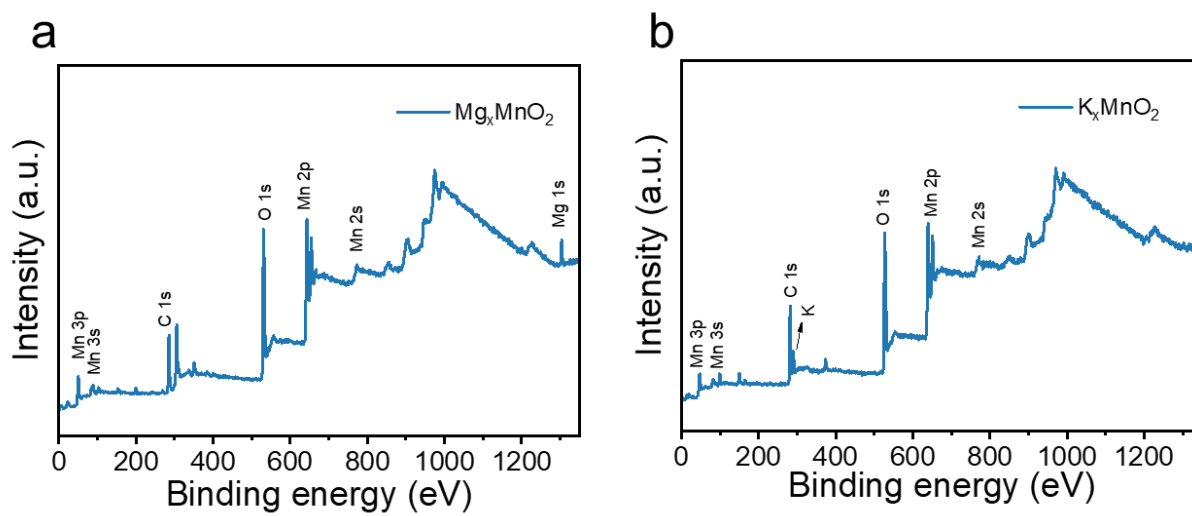


**Figure S2.** Survey XPS spectra of pristine a)  $Mg_xMnO_2$  and b)  $K_xMnO_2$ .

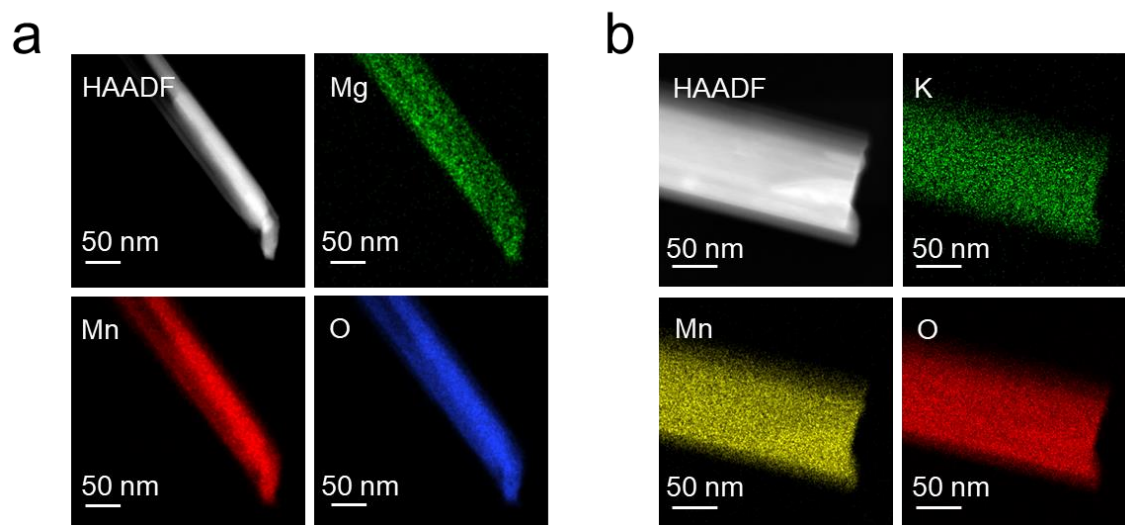


**Figure S3.** EDS mapping images of a)  $\text{Mg}_x\text{MnO}_2$  and b)  $\text{K}_x\text{MnO}_2$ . Mn, O, Mg elements are evenly distributed in  $\text{Mg}_x\text{MnO}_2$  and Mn, O, K elements are distributed homogeneously in  $\text{K}_x\text{MnO}_2$ , which match well with XPS measurement.

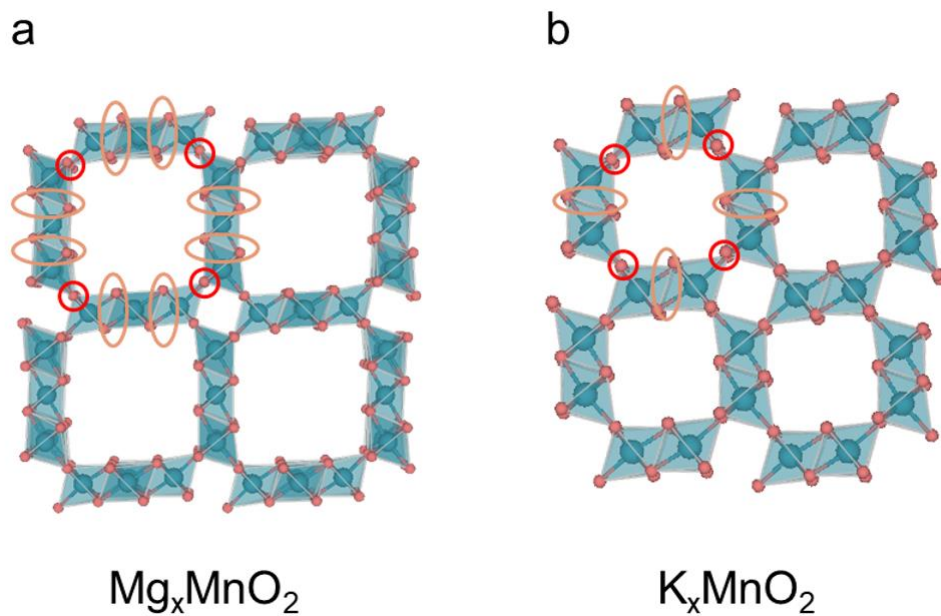


**Figure S4.** Crystal structure of a)  $\text{Mg}_x\text{MnO}_2$  and b)  $\text{K}_x\text{MnO}_2$ . The  $\text{Mg}_x\text{MnO}_2$  has more corner-sharing  $[\text{MnO}_6]$  octahedra than  $\text{K}_x\text{MnO}_2$ .

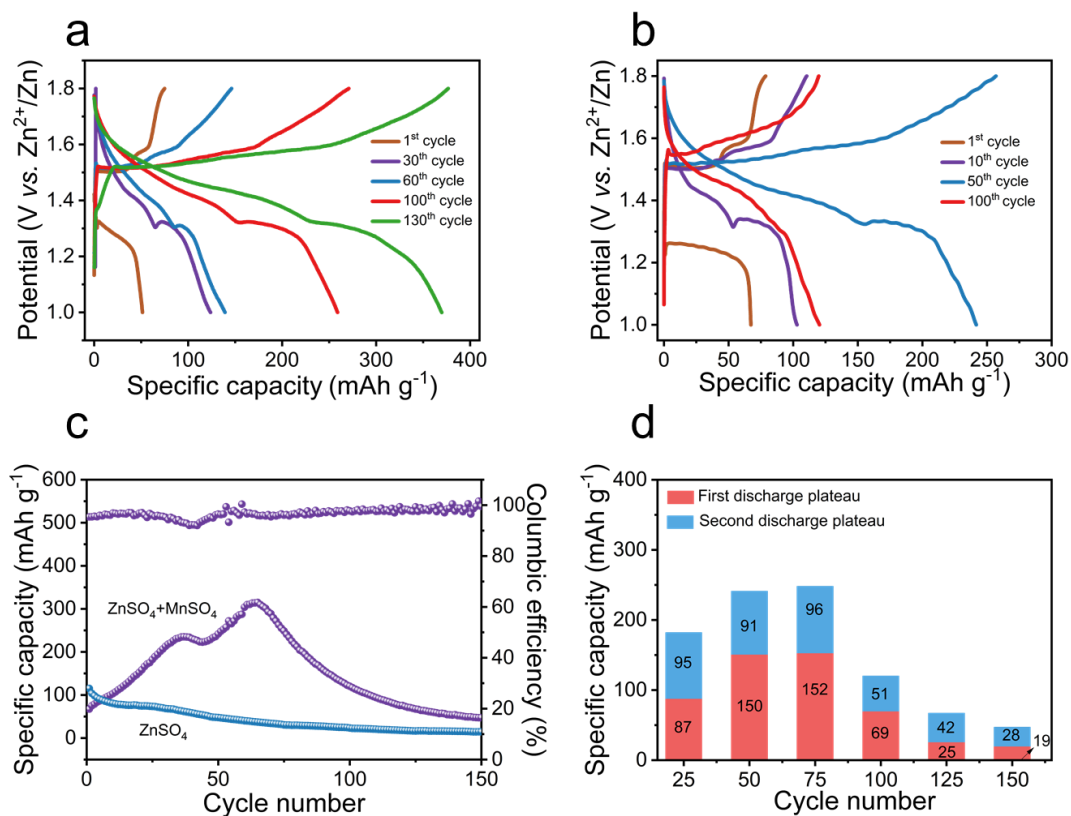


**Figure S5.** Galvanostatic charge-discharge curves at  $100 \text{ mA g}^{-1}$  for different cycles of a)  $\text{Mg}_x\text{MnO}_2$  and b)  $\text{K}_x\text{MnO}_2$ . c) Cycling performance of  $\text{K}_x\text{MnO}_2$  at  $100 \text{ mA g}^{-1}$  with  $2 \text{ M ZnSO}_4 + 0.2 \text{ M MnSO}_4$  and  $2 \text{ M ZnSO}_4$ , respectively. d) Quantitative first and second plateau contribution to capacity delivery in different cycles of  $\text{K}_x\text{MnO}_2$ .

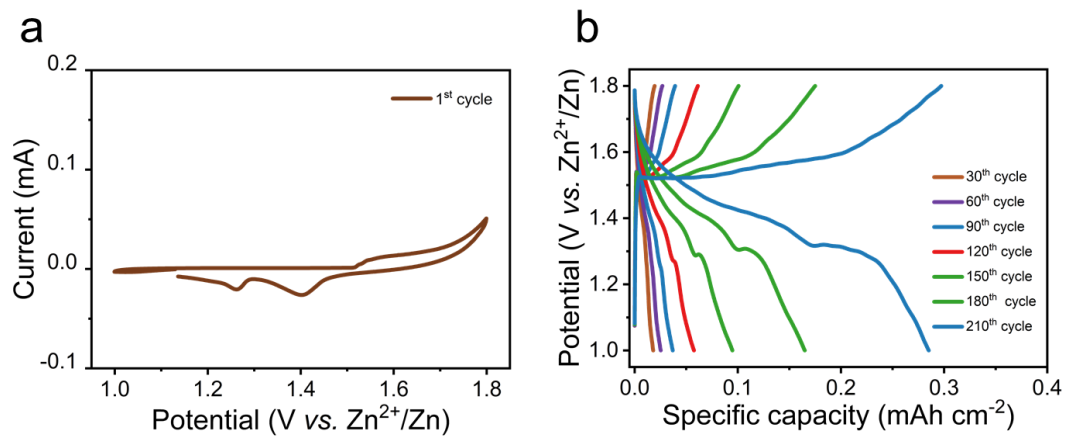


**Figure S6.** a) CV curves of carbon paper at the first cycle with 2 M ZnSO<sub>4</sub> + 0.2 M MnSO<sub>4</sub>, at the scan rate of 0.1 mV s<sup>-1</sup>. b) Galvanostatic charge-discharge curves at 100 mA g<sup>-1</sup> for different cycles of carbon paper.

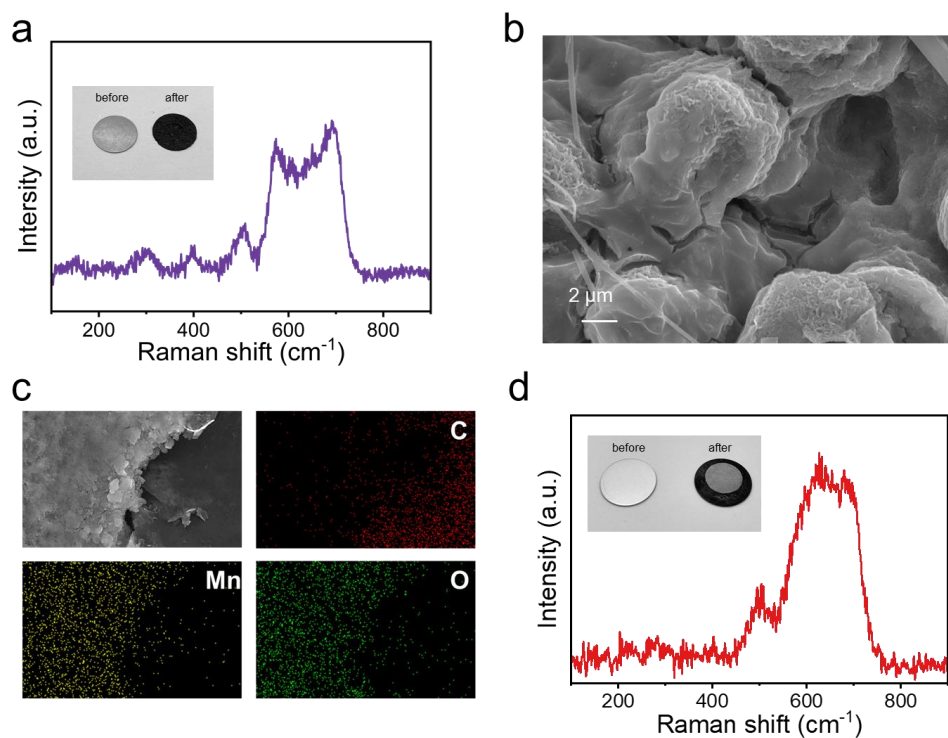


**Figure S7.** a) Raman spectra, b) SEM image and c) EDS mapping of carbon paper at the charged state. d) Raman spectrum of steel sheet after 250 cycles. After 250 cycles, the carbon paper turns to black. This new thick layer grown on the carbon paper was observed by SEM image in Figure S7b, and the Mn, O elements are evenly distributed on it (Figure S7c). This new layer of materials may be a kind of manganese oxides. In Figure S7d, the manganese oxide covered the surface of electrode and can also be found at steel sheet after 250 cycles which may be one of the reasons of the capacity fading.

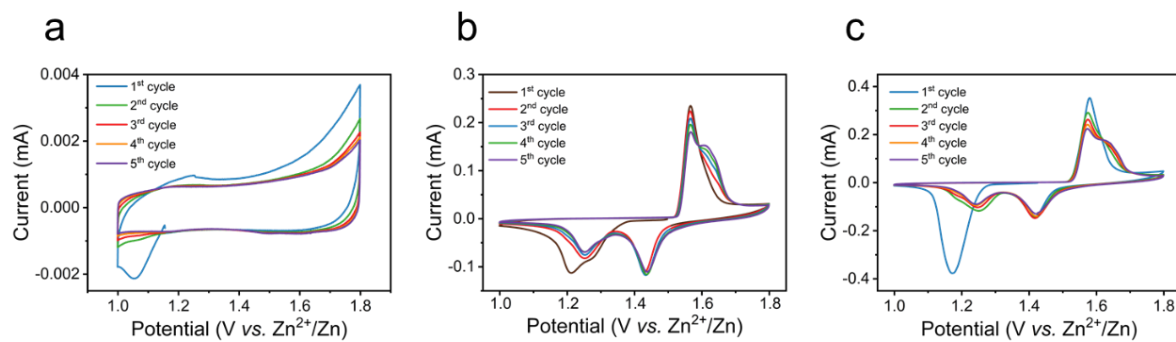


**Figure S8.** CV curves of a) carbon paper, b)  $\text{Mg}_x\text{MnO}_2$ , c)  $\text{K}_x\text{MnO}_2$  in  $\text{ZnSO}_4$  electrolyte,

from 1.0 V to 1.8 V versus  $\text{Zn}^{2+}/\text{Zn}$  at a scan rate of  $0.1 \text{ mV s}^{-1}$ , respectively.

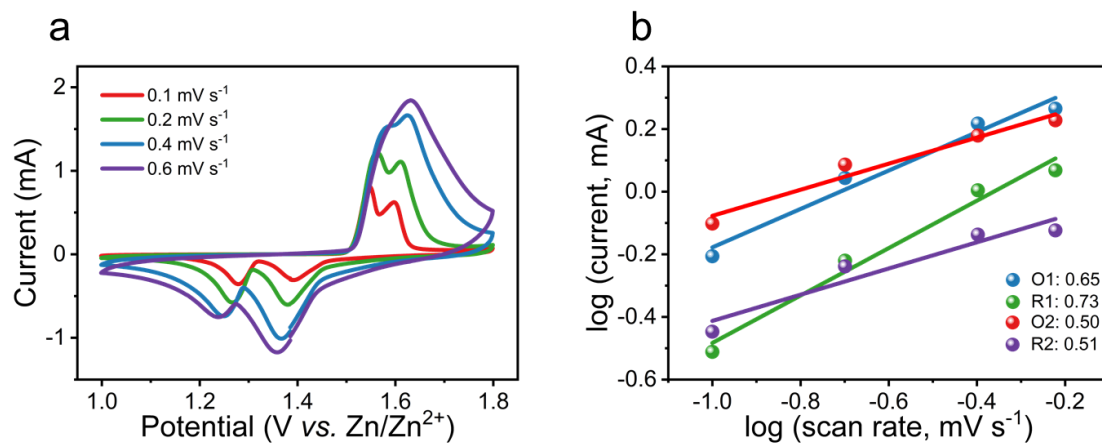


**Figure S9.** a) CV curves at the scan rates ranging from 0.1 to 0.6  $mV s^{-1}$ . b) Log (i) versus log (v) plots at different oxidation and reduction states based on CV curves of  $K_xMnO_2$ .

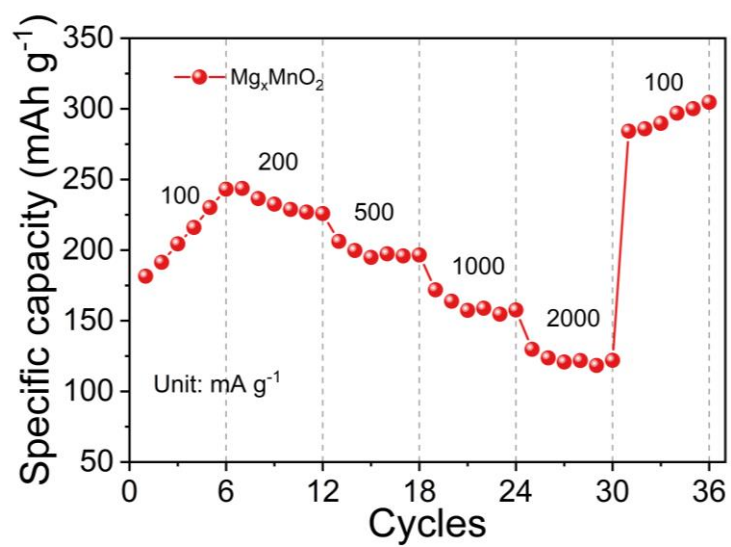


**Figure S10.** Rate capability from 100 mA g<sup>-1</sup> to 2000 mA g<sup>-1</sup> of  $\text{Mg}_x\text{MnO}_2$ .

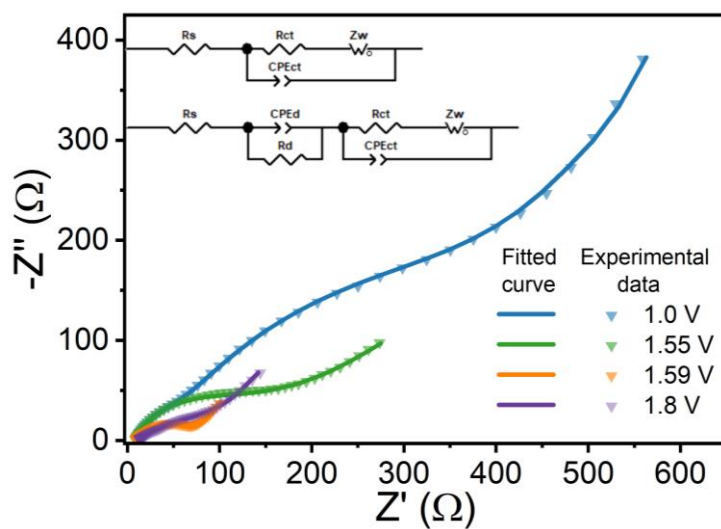


**Figure S11.** Nyquist plots of experimental data and fitting curves of  $\text{Mg}_x\text{MnO}_2$  at different potential states.

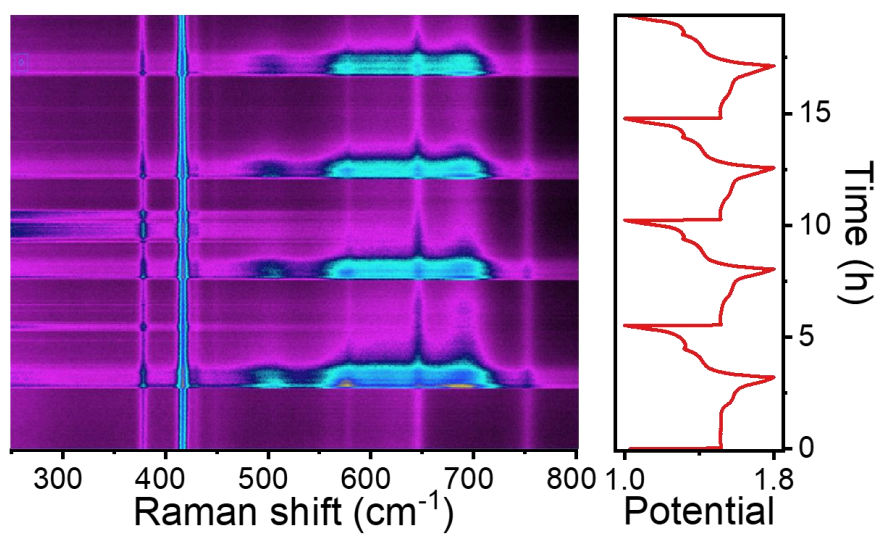


**Figure S12.** In-situ Raman spectra of  $\text{Mg}_x\text{MnO}_2$  nanowires.

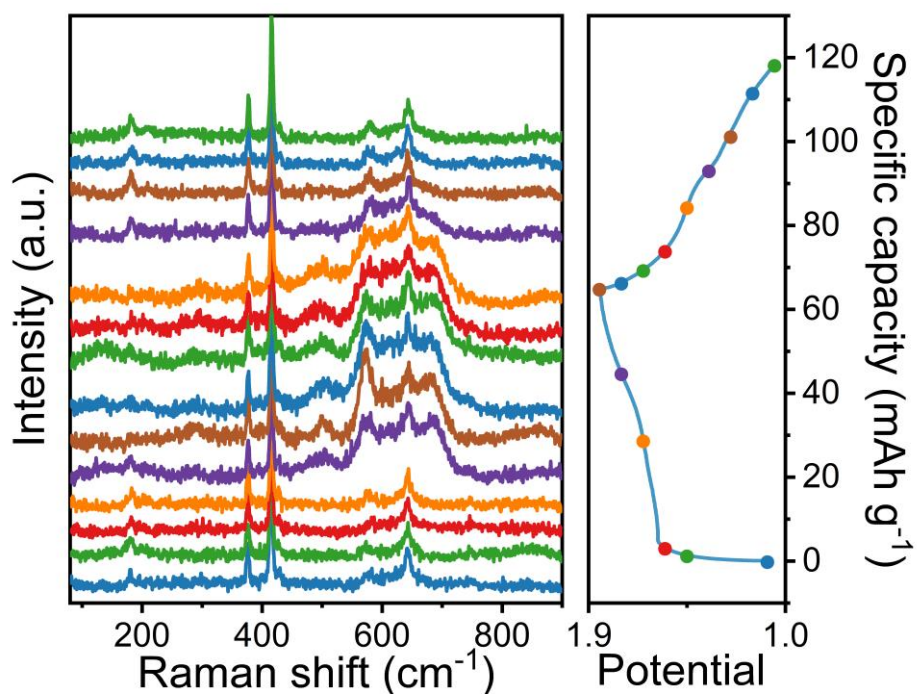


**Figure S13.** In-situ Raman spectra of  $K_xMnO_2$  and the corresponding galvanostatic charge and discharge curves at  $100 mA g^{-1}$ .

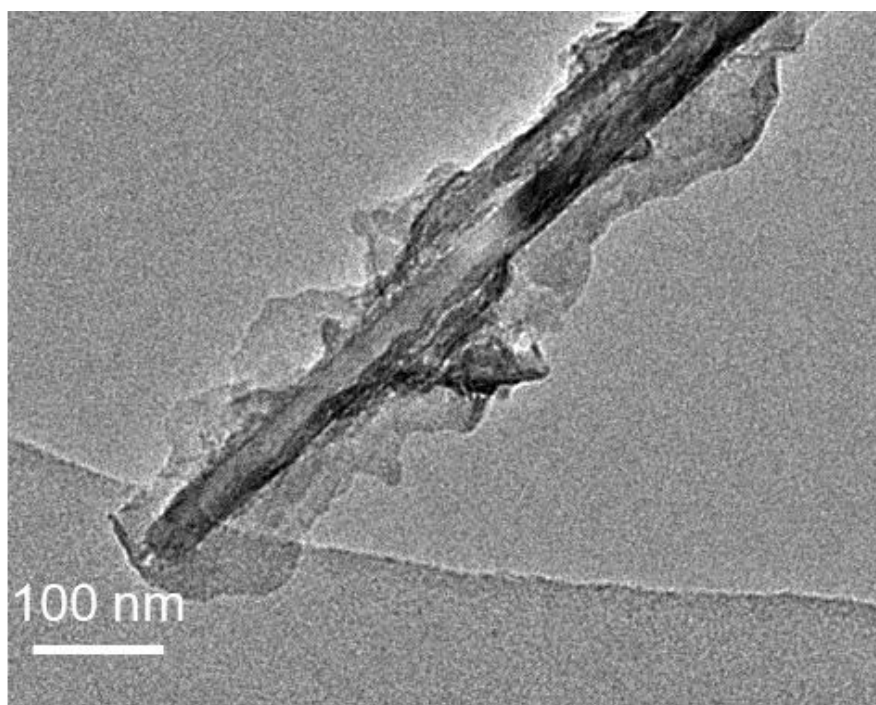


**Figure S14.** TEM image of Mg<sub>x</sub>MnO<sub>2</sub> nanowire after cycling.

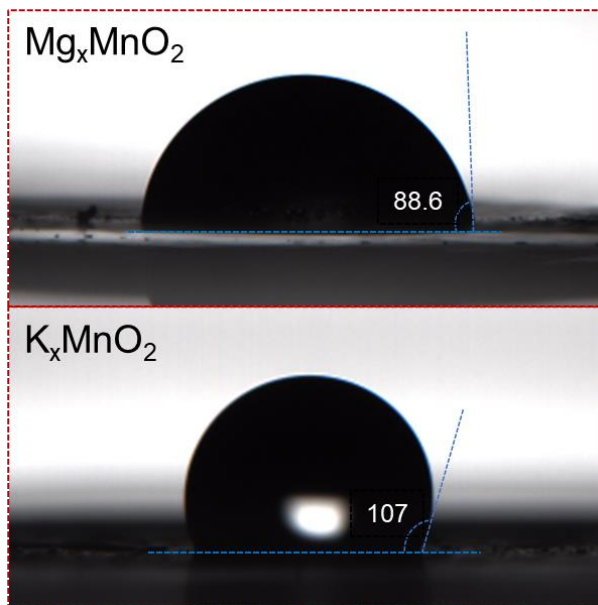


**Figure S15.** Contact angles of droplets on Mg<sub>x</sub>MnO<sub>2</sub> and K<sub>x</sub>MnO<sub>2</sub> nanowire surface. The contact angle is 86° for Mg<sub>x</sub>MnO<sub>2</sub> which means that Mg<sub>x</sub>MnO<sub>2</sub> nanowire has better wettability.

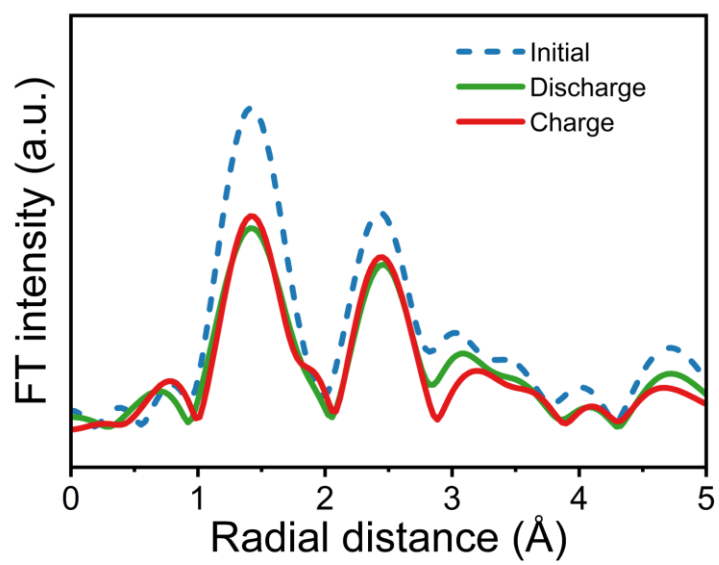


**Figure S16.** Mn K-edge EXAFS spectra of  $K_xMnO_2$  at different states.

**Reference**

- [1] B. Ravel, M. Newville, *J. Synchrotron Rad.* **2005**, 12, 537.